VERSITA

Cent. Eur. J. Chem. • 8(1) • 2010 • 96–107
DOI: 10.2478/s11532-009-0103-2

Central European Journal of **Chemistry**

Synthesis, characterization and biological activities of homo-binuclear Cu(II) and Zn(II) complexes derived from 2-hydroxy-5-methyl-1,3-benzenedicarboxaldehyde derivatives

Research Article

Natarajan Raman*, Arumugam Sakthivel, Ramaraj Jeyamurugan

Research Department of Chemistry, VHNSN College, Virudhunagar-626001, India

Received 30 April 2009; Accepted 17 July 2009

Abstract: Few novel binuclear Schiff base metal complexes [M_2LCl_3], where M = Cu(II) and Zn(II); L= 2,6-bis-({2-[(3-hydroxy-4-nitrobenzylidene)amino]ethylimino}methyl)-4-methylphenol (BHEM), 2,6-bis-({2-[(3,4-dimethoxybenzylidene)amino]ethylimino}methyl)-4-methylphenol (BDEM) and 2,6-bis-({2-[(2,3,5-trichlorobenzylidene)amino]ethylimino}methyl)-4-methylphenol (BTEM), have been synthesized and characterized by analytical and spectral data. The data suggest that BHEM/BDEM/BTEM ligands afford square-pyramidal/distorted square-pyramidal geometry on metalation with Zn(II)/Cu(II). The binding behaviour of these complexes with DNA has been investigated using electronic absorption spectroscopy as well as viscosity and voltammetric measurements; the results show that they interact with DNA through intercalating way. From the DNA cleavage study of these complexes, investigated by gel electrophoresis, we found that they efficiently cleave supercoiled pUC19 DNA in the presence of a reducing agent (3-mercaptopropionic acid) and on irradiation with UV light of 360 nm wavelength. The mechanism reveals that singlet oxygen ($^1O_2$) plays a significant role in the photo cleavage. The superoxide dismutase (SOD) mimetic activity of the synthesized complexes demonstrates that most of the complexes have promising SOD-mimetic activity. The antimicrobial study indicates that the complexes inhibit the growth of bacteria and fungi more than the free ligands.

Keywords: *Binuclear complexes • Photo cleavage • DNA binding • SOD activity*

1. Introduction

The design and synthesis of binucleating ligands and their complexes has been of much interest in the recent past [1]. The studies done on binuclear metal complexes in which the two metal centers are held in close proximity have addressed [2,3] the ligand environment, redox behaviour, magnetic exchange interactions and spectroscopic properties. Considerable interest has also been placed on synthesis and biomimetic reactions of model systems related to metalloenzymes [4]. In the area of development of artificial nucleases researchers are interested in designing multimetal models [5,6]; complexes with polyaza ligands are of special interest due their high DNA cleavage activity [7,8].

DNA cleavage by metal complexes generally occurs *via* oxidative and hydrolytic pathways [9,10]. The oxidative DNA cleavage involves abstraction of sugar hydrogen atom and/or damage of DNA by nucleobase oxidation whereas hydrolytic cleavage involves hydrolysis of the phosphodiester bond. The photo-activated oxidative cleavage of DNA has recently received considerable attention due to its utility in highly targeted photo-chemotherapeutic applications. For example porphyrin

* *E-mail: drn_raman@yahoo.co.in*

and phthalocyanin-based compounds have found clinical applications in photodynamic therapy (PDT) of cancer [11,12]. Among the non-porphyrinic species, the DNA photo-cleavage activity of 4d and 5d metal complexes has been studied in detail [13,14]. In comparison, the chemistry of 3d metal based model photonuclease has remained relatively unexplored [15,16]. Hence, in this work we report the synthesis, characterization, and antimicrobial, DNA binding and DNA cleavage activities of binuclear Cu(II) and Zn(II) complexes having tertraaza ligands.

2. Experimental procedure

2.1. Materials and Methods

All reagents and chemicals were procured from Merck products. Solvents used in electrochemical and spectroscopic studies were purified using standard procedures [17]. DNA was purchased from Bangalore Genei (India). Agarose (molecular biology grade) and ethidium bromide were obtained from Sigma (USA). C, H and N analyses of the complexes were carried out on a CHN analyzer Calrlo Erba 1108, Heraeus. The IR (KBr discs) of the samples was recorded on a Perkin–Elmer 783 series FTIR spectrophotometer. The UV-Vis, spectra of the samples were recorded on a Shimadzu UV-1601 spectrophotometer. ^{1}H and ^{13}C NMR spectra (300 MHz) of the ligands and their zinc complexes were recorded on a Bruker Avance DRX 300 FT-NMR spectrometer in $CDCl_3$ and DMSO-d_6 respectively using trimethylsilane (TMS) as the internal standard. The fast atom bombardment (FAB) mass spectra of the complexes were recorded on a JEOL SX 102/DA-6000 mass spectrometer using Argon/Xenon (6 kV, 10 mA) as the FAB gas. The accelerating voltage was 10 kV and the spectra were recorded at room temperature using *m*-nitrobenzyl alcohol as the matrix. Molar conductance of 10^{-3}M solution of the complexes in N,N-dimethylformamide (DMF) was measured at room temperature with an Deepvision Model-601 digital direct reading deluxe conductivity meter. Magnetic susceptibility measurements were carried out by employing the Gouy method at room temperature on powder sample of the complex using $CuSO_4 \cdot 5H_2O$ as the calibrant. Electrochemical measurements were performed on a CHI 620C electrochemical analyzer. The purity of ligands and their complexes was evaluated by column and thin layer chromatography.

2.2. Estimation of metal

The metals, in general, were estimated gravimetrically as their oxides [18] by fusion with AnalaR ammonium oxalate. In a typical experiment, about 0.3 g of the dried complex was accurately weighed in a previously weighed silica crucible. AnalaR ammonium oxalate, roughly 3 parts by weight of the complex was added and the mixture was incinerated slowly at first and then more vigorously using a Bunsen burner for 3 h. It was then cooled in a desiccator and weighed. The procedure was repeated till the final weight of the oxide was constant. The percentage of metal in the complex was calculated from the weight.

2.3. Synthesis of ligands

The precursor (2-hydroxy-5-methyl-1,3-benzenedicarboxaldehyde) was synthesized by the method described in [19]. The outline of the synthesis of the ligands using this precursor is shown in Scheme 1.

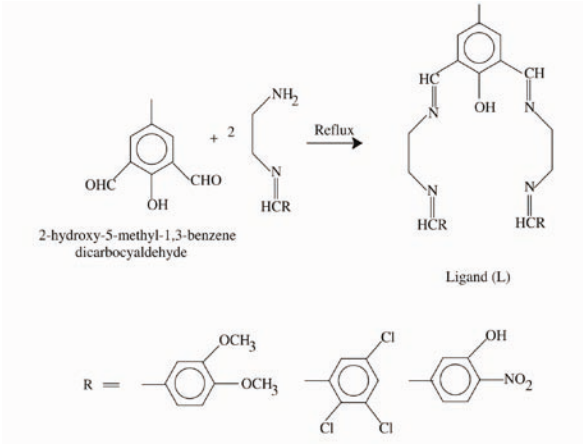

Scheme 1. The outline of the synthesis of the ligands

2.3.1. Preparation of N´-(3,4-dimethoxybenzylidene) ethane-1,2-diamine

An ethanolic solution (20 mL) of ethylenediamine (0.60 g; 10 mM) was slowly added, with stirring, to an ethanolic solution (40 mL) of 3,4-dimethoxybenzaldehyde (1.67 g; 10 mM). The mixture was refluxed for 1 h and then the clear solution was allowed to cool to room temperature. The solid material formed was removed by filtration and recrystallised from EtOH.

N´-(2,3,5-trichlorobenzylidene)ethane-1,2-diamine and N´-(3-hydroxy-4-nitrobenzylidene) ethane-1,2-diamine were synthesized according to the procedure described above by the replacement of 3,4-dimethoxybenzaldehyde by 2,3,5-trichlorobenzaldehyde (2.09 g; 10 mM) and 3-hydroxy-4-nitrobenzaldehyde (1.67 g; 10 mM), respectively.

2.3.2. Synthesis of BDEM ligand

N´-(3,4-dimethoxybenzylidene)ethane-1,2-diamine (2.08 g; 10 mM) and 2-hydroxy-5-methyl-1,3-

benzenedicarboxaldehyde (0.82 g; 5 mM) were refluxed for 3 h in ethanolic solution (40 mL). The pale yellow precipitate that crystallized out from the clear solution upon cooling was filtered off, washed with EtOH and dried in *vacuo*. Yield: 1.85 g; (64%). IR (KBr, cm^{-1}): 2855 (methyl $–CH_3$), 1628 (–CH=N), 3250-3500 (–OH). ^{1}H-NMR ($CDCl_3$): (phenyl multiplet) 6.6-7.5 δ, ($–OCH_3$) 3.8 δ, ($–CH_3$) 2.2 δ, ($–CH_2–$) 3.4 δ (t, J = 7.25 Hz, 4H), (–OH) 12.3 δ, (–CH=N–) 8.3 δ; m/z: 546; Anal. Calcd for [$C_{31}H_{37}N_4O_5$]: C, 68.3, H, 6.8, N, 10.2; Found: C, 67.7, H 6.7, N. 9.7 (%); UV-visible [$\lambda_{max,}$ nm, (ε, $dm^3\ mol^{-1}\ cm^{-1}$)] in EtOH, 272 (32740) and 384 (11789).

Ligands BHEM and BTEM were synthesized according to the procedure described above by the replacement of N´-(3,4-dimethoxybenzylidene)ethane-1,2-diamine by N´-(3-hydroxy-4-nitrobenzylidene) ethane-1,2-diamine (2.89 g; 10 mM) and N´-(2,3,5-trichlorobenzylidene)ethane-1,2-diamine (2.51 g; 10 mM), respectively. BHEM: Yield: 1.92 g; (52%). IR (KBr, cm^{-1}): 3250-3500 (–OH), 1365 ($– NO_2$), 1635 (–CH=N), 2834 (methyl $–CH_3$), ^{1}H-NMR ($CDCl_3$): 6.4-7.6 δ (phenyl multiplet), ($–CH_3$) 2.2 δ, ($–CH_2–$) 3.4 δ (t, J = 2.5 Hz, 4H), (–OH) 11.1 δ, (–OH) 12.4, (–CH=N–) 7.9 δ; m/z: 548: Anal. Calcd for [$C_{27}H_{26}N_6O_7$]: C, 59.3, H, 4.8, N, 15.4; Found: C, 58.4, H, 4.8, N, 14.9 (%); UV-visible [$\lambda_{max,}$ nm, (ε, $dm^3\ mol^{-1}\ cm^{-1}$)] in EtOH, 284 (29758) and 379 (14589). BTEM: Yield: 2.47 g; (75%). IR (KBr, cm^{-1}): 3250-3500 (–OH), 1631 (–CH=N), 2858 (methyl–CH_3); ^{1}H-NMR ($CDCl_3$): (phenyl multiplet) 6.4-7.6 δ, ($–CH_3$) 2.2 δ, ($–CH_2–$) 3.3 δ (t, J = 4.8 Hz, 4H), (–CH=N–) 8.2 δ; m/z: 631; Anal. Calcd for [$C_{27}H_{22}N_4OCl_6$]: C, 51.4, H, 3.5, N, 8.9; Found: C, 50.5, H, 3.5, N, 8.4 (%); UV-visible [$\lambda_{max,}$ nm, (ε, $dm^3\ mol^{-1}\ cm^{-1}$)] in EtOH, 275 (31458) and 387 (15438).

2.3.3. Synthesis of [Cu_2(BDEM)Cl_3] complex

Copper(II) chloride (1.72 g; 10 mM) in EtOH (30 mL) was added, with stirring, to an ethanolic solution (40 mL) of the BDEM (2.73 g; 5 mM) and refluxed for 3 h. The dark green compound that precipitated was filtered off, washed with EtOH and dried in *vacuo*. Yield: 2.31 g; (52 %). IR (KBr): 2860 (methyl $–CH_3$), 1601 (–CH=N), 489 (M–O), 420 (M–N) and 249 (M–Cl) cm^{-1}. m/z: 778, Anal. Calcd for [$Cu_2C_{31}H_{36}N_4O_5Cl_3$] : Cu, 16.3, C, 47.8, H, 4.6, N, 7.2: Found: Cu, 15.8, C, 47.2, H, 4.6, N, 7.1 (%). $\lambda_M\ 10^{-3}$ ($ohm^{-1}\ cm^2\ mol^{-1}$) 7.7; μ_{eff} (BM), 1.08. UV-visible [$\lambda_{max,}$ nm, (ε, $dm^3\ mol^{-1}\ cm^{-1}$)] in DMF, 274 (31452), 343.5 (11235), 452 (19785) and 642 (110); IC_{50}, 45 µmol/ dm^{-1}.

Similarly, complexes [Cu_2(BHEM)Cl_3] and [Cu_2(BTEM)Cl_3] were synthesized according to the procedure described above. [Cu_2(BHEM)Cl_3]: Yield: 3.07 g; (69%). IR (KBr, cm^{-1}) : 3250-3500 (–OH), 1368 ($– NO_2$), 1598 (–CH=N), 2838 (methyl $–CH_3$), 497 (M–O), 428 (M–N) and 282 (M–Cl) m/z: 780, Anal. Calcd for [$Cu_2C_{27}H_{25}N_6O_7Cl_3$] : Cu, 16.3, C, 41.6, H, 3.2, N, 10.8: Found: Cu, 15.6, C, 41.1, H, 3.3, N 10.1(%). $\lambda_M\ 10^{-3}$ ($ohm^{-1}\ cm^2\ mol^{-1}$), 10.4; μ_{eff} (BM), 1.48. UV-visible [$\lambda_{max,}$ nm, (ε, $dm^3\ mol^{-1}\ cm^{-1}$)] in DMF, 262 (28459), 355.5 (12983) and 628 (179); IC_{50}, 31 µmol/ dm^{-1}. [Cu_2(BTEM)Cl_3]: Yield: 2.87 g; (59 %). IR (KBr, cm^{-1}): 1605 (–CH=N), 2862 (methyl–CH_3), 485 (M–O), 441 (M–N), 271 (M–Cl); m/z: 864, Anal. Calcd for [$Cu_2C_{27}H_{21}N_4OCl_9$] : Cu, 14.7, C, 37.5, H, 2.4, N, 6.4; Found: Cu, 14.2, C, 37.1, H 2.4, N, 5.9(%). $\lambda_M\ 10^{-3}$ ($ohm^{-1}\ cm^2\ mol^{-1}$), 7.8; μ_{eff} (BM), 0.98. UV-visible [$\lambda_{max,}$ nm, (ε, $dm^3\ mol^{-1}\ cm^{-1}$)] in DMF, 260 (27451), 363 (10789) and 647 (174), IC_{50}, 27 µmol/ dm^{-1} .

2.3.4. Synthesis of zinc complexes

Zinc chloride (1.36 g; 10mM) in EtOH (40 mL) was added, with stirring, to an ethanolic solution (40 mL) of the ligand (BDEM) (2.73 g; 5 mM) and refluxed for 2 h. The dirty white compound that precipitated was filtered off, washed with EtOH and dried in *vacuo*. Yield: 1.68 g; (41%). IR (KBr, cm^{-1}): 2855 (methyl–CH_3), 1602 (–CH=N), 471 (M–O), 445 (M–N), 285 (M–Cl). ^{1}H-NMR (DMSO-d_6): (phenyl multiplet), 6.6-7.5 δ, ($–OCH_3$) 3.8 δ, ($–CH_3$) 2.2 δ, ($–CH_2–$) 3.4 δ (t, J = 8.1 Hz, 4H), (–CH=N–), 8.1 δ; m/z: 782. Anal. Calcd for [$Zn_2C_{31}H_{36}N_4O_5Cl_3$] : Zn, 16.7, C, 47.6, H, 4.6, N 7.1: Found: Zn 16.1, C 47.4, H 4.6, N, 6.8(%). $\lambda_M\ 10^{-3}$ ($ohm^{-1}\ cm^2\ mol^{-1}$), 6.2 UV-visible [$\lambda_{max,}$ nm, (ε, $dm^3\ mol^{-1}\ cm^{-1}$)] in DMF, 254 (28758) and 340 (14358), IC_{50}, 74 µmol/ dm^{-1}.

Similarly, complexes [Zn_2(BHEM)Cl_3] and [Zn_2(BTEM)Cl_3] were synthesized according to the procedure described above. [Zn(BHEM)Cl_3]: Yield: 1.43 g; (35%). IR (KBr, cm^{-1}): 3250-3500 (–OH), 1371 ($– NO_2$), 1609 (–CH=N), 2824 (methyl–CH_3), 494 (M–O), 430 (M–N), 288 (M–Cl). ^{1}H-NMR (DMSO-d_6): (phenyl multiplet) 6.4-7.6 δ, ($–CH_3$) 2.2 δ, ($–CH_2–$) 3.4 δ (t, J = 2.8 Hz, 4H), (–OH) 11.1 δ, (–CH=N–) 7.9 δ; m/z: 784 Anal. Calcd for [$Zn_2C_{27}H_{25}N_6O_7Cl_3$] : Zn, 16.7, C, 41.4, H, 3.2, N, 10.7: Found: Zn, 15.9, C, 40.7, H, 3.3, N, 10.4(%). $\lambda_M\ 10^{-3}$ ($ohm^{-1}\ cm^2\ mol^{-1}$), 11.9; UV-visible [$\lambda_{max,}$ nm, (ε, $dm^3\ mol^{-1}\ cm^{-1}$)] in DMF, 242 (17248), 352 (6331), IC_{50}, 72 µmol/ dm^{-1}: [Zn_2(BTEM)Cl_3]: Yield: 1.94 g; (43 %). IR (KBr, cm^{-1}): 1602 (–CH=N), 2842 (methyl–CH_3), 492 (M–O), 447 (M–N) and 275 (M–Cl); ^{1}H-NMR (DMSO-d_6): (phenyl multiplet) 6.4-7.6 δ, ($–CH_3$) 2.2 δ, ($–CH_2–$) 3.3 δ (t, J = 5.1 Hz, 4H), (–CH=N–) 8.0 δ; m/z: 867; Anal. Calcd for [$Zn_2C_{27}H_{21}N_4OCl_9$] : Zn, 15.0, C, 37.3, H, 2.4, N, 6.4: Found: Zn, 14.6, C, 36.9, H, 2.4, N, 6.1 (%). $\lambda_M\ 10^{-3}$ ($ohm^{-1}\ cm^2\ mol^{-1}$), 12.4; UV-visible [$\lambda_{max,}$ nm, (ε, $dm^3\ mol^{-1}\ cm^{-1}$)] in DMF, 262 (21498), 367 (9507), IC_{50}, 58 µmol/ dm^{-1}.

2.4. DNA binding study

The binding of complexes to DNA using electronic absorption, electrochemical, and viscosity measurements was done according to the methods described in [20].

2.5. DNA cleavage study

The extent of cleavage of super coiled (SC) pUC19 DNA (33.3 μM, 0.2 μg) to its nicked circular (NC) form was determined by agarose gel electrophoresis in 50 mM Tris–HCl buffer (pH 7.2) containing 50 mM NaCl. For photo-induced DNA cleavage studies, the reactions were carried out under illuminated conditions using UV sources at 360 nm. After exposure to light, each sample was incubated for 1 h at 37°C and analyzed for the photo-cleaved products using gel electrophoresis as discussed below. The inhibition reactions for the "chemical nuclease" reactions were carried out under dark conditions by adding the reagents (distamycin 50 μM and DMSO 4 μL) prior to the addition of each complex and the reducing agent, 3-mercaptopropionic acid (MPA). The inhibition reactions for the photo-induced DNA were carried out at 360 nm adding the reagents (NaN_3 100 μM and DMSO 4 μL) prior to the addition of each complex. For the D_2O experiment, the solvent (D_2O) was used for the dilution of the sample to 18 μL. The samples, after incubation for 1 h at 37°C in a dark chamber, were added to the loading buffer containing 25% bromophenol blue, 0.25% xylene cyanol and 30% glycerol (3 μL) and the solution was finally loaded on 0.8% agarose gel containing 1 μg mL^{-1} ethidium bromide. Electrophoresis was carried out in a dark chamber for 3 h at 50V in Tris-acetate-EDTA buffer. Bands were visualized by UV light and photographed.

2.6. Antimicrobial activity

The *in vitro* biological screening effects of the investigated compounds were tested against the bacteria *Salmonella typhi, Staphylococcus aureus, Escherichia coli,* and *Bacillus subtilis* by the disc diffusion method, using agar nutrient as the medium and streptomycin as the standard. The antifungal activities of the compounds were evaluated by the disc diffusion method against the fungi *viz*., *Aspergillus niger, Aspergillus flavus, Candida Albicans* and *Rhizoctonia bataicola* cultured on potato dextrose agar as medium and nystatin as the standard. The stock solution (10^{-2} M) was prepared by dissolving the compounds in DMSO and the solutions were serially diluted in order to find the minimum inhibitory concentration (MIC) values. In a typical procedure [21], the disc was filled with the test solution using a micropipette and the plate was incubated 24 h for bacteria and 72 h for fungi at 35°C. During this periodthe test solution diffused and the growth of the inoculated microorganisms was affected. The inhibition zone was developed, at which the concentration was noted.

2.7. Superoxide dismutase activity

The superoxide dismutase activity of the complexes was assayed using nitrobluetetrazolium chloride (NBT) as reported previously [22]. The concentration of the complex required to yield 50% inhibition of the reduction of NBT (named IC_{50}) was determined.

3. Results and Discussion

The ligands (L) and their complexes are found to be stable in air. The ligands are soluble in common organic solvents but the complexes are soluble only in DMF and DMSO. The elemental analytical and mass spectral data of the ligands and their complexes are in agreement with the formulae $[M_2LCl_3]$. The magnetic moment of Cu(II) complexes lie in the range 0.98-1.48 BM at room temperature. The observed magnetic moment values are less than the spin only value (1.73 to 2.20 BM) for Cu(II) ($3d^9$) mononuclear complexes having no major interactions between the moieties. The low magnetic moments in Cu(II) complexes are usually attributed to spin-coupling within a dimer brought about by the bridging of monomeric units of paramagnetic centers through the phenolic oxygen or chlorine atoms. This oxygen or chlorine bridging often leads to change in electronic structure of the attached atoms resulting in reduction of paramagnetism, partially or completely, of the metal atoms bridge. Hence the subnormal magnetic moments observed for the studied Cu(II) complexes may be accounted for by assuming a dimeric structure in the solid state, in which a considerable antiferromagnetic exchange occurs through a super exchange mechanism as there is little possibility of a direct interaction.

The IR spectra of the ligands exhibit a strong band at 1624-1635 cm^{-1} assigned to ν(C=N) stretching frequency. This band shifts to lower wave numbers (~25 cm^{-1}) in all the complexes, suggesting the coordination of the azomethine nitrogen to the metal centre [23]. The phenolic ν(OH), found as a weak broad band in the 3250-3500 cm^{-1} region, disappears in all complexes indicating deprotonation and coordination to the metal. This is further supported by the shift of phenolic ν(C–O) from 1280 cm^{-1} recorded for the ligands to higher frequency, by about 40-50 cm^{-1}, in complexes. The low frequency bands in the 500-470 and 420-450 cm^{-1} regions are assigned to ν(M-O) and ν(M-N) respectively [24]. The presence of a chloro bridge is evident from the IR bands observed in the 290-240 cm^{-1} region. The ligand (BHEM) gives a broad band for the

–OH group at *ca*. 3250-3500 cm^{-1}, which is attributable to the phenolic –OH group present in the 3-hydroxy-4-nitrobenzaldehyde moiety. The appearance of this peak in their copper and zinc complexes indicates that the chelation does not take place via the –OH group.

In general typical Cu(II) complexes of square-pyramidal or distorted square-pyramidal geometries exhibit a band in the 550-650 nm range [25-26]. The electronic absorption spectra of the Cu(II) complexes, recorded in DMF solution, show one broad band in the visible region around 628-647 nm, which is assigned to distorted-square pyramidal geometry around the Cu(II) ion.

The decoupled ^{13}C NMR spectra of BDEM (in $CDCl_3$) and its zinc complex (in DMSO-d_6) confirm the presence of azomethine (-C=N-) and methoxy (–OCH_3) groups. In the zinc complex, the imine carbon signal was deshielded compared to the free ligand suggesting the coordination of azomethine nitrogen to the metal ion. Comparison of all other macrocyclic carbon peaks of the ligand with those of the zinc complex [Zn_2LCl_3] shows some up-field and down-field shifts which are not very significant. The data for the free ligand and its zinc complex given in Table 1 are in good agreement with the assigned structure of the ligand and its complex.

Based on the above spectral and analytical data, the structure of the Schiff base complexes is given in Fig. 1.

3.1. DNA binding studies

3.1.1. Absorption titration

The electronic absorption spectrum of copper complex [Cu_2(BDEM)Cl_3] in the presence of increasing amounts of CT DNA in 5 mM Tris-HCl and 50 mM NaCl buffer (pH 7.2) is shown in Fig. 2. In the UV region, the intense absorption bands observed in the region 340-367 nm were attributed to intra ligand π-π* transition. Increase in concentration of CT-DNA resulted in the hypochromism and blue-shift in UV-Vis spectrum of the copper complex. These spectral characteristics suggest that the copper complex might bind to DNA by an intercalative mode due to a strong stacking interaction between the aromatic chromophore of the complex and the base pairs of the DNA. After intercalating the base pairs of DNA, the π*orbital of the intercalated ligand could couple with the π orbital of the base pairs, thus decreasing the π-π*transition energy and further resulting in the blue-shift. On the other hand, the coupling of the π orbital was partially filled by electrons, thus decreasing the transition probabilities and concomitantly, resulting in the hypochromism. A similar type of binding mode was observed for other complexes with CT DNA. In order to compare the binding strength of the complexes with CT DNA, the intrinsic binding constants, K_b (Table 2), are obtained by monitoring the changes in the absorbance for the complexes with increasing concentration of DNA.

Table 1. ^{13}C- NMR spectral data (ppm) of ligand (BDEM) and its Zn(II) complex

Assignment	Ligand (BDEM)	Zn complex
C_1	21.4	21.4
C_2	131.1	131.1
C_3	133.7	133.7
C_4	128.5	128.5
C_5	164.4	163.7
C_6	49.2	49.1
C_7	45.9	45.5
C_8	161.4	161.1
C_9	129.6	129.4
C_{10}	113.4	113.2
C_{11}	154.2	145.1
C_{12}	148.8	148.6
C_{13}	110.2	110.2
C_{14}	121.6	122.4
C_{15}	54.7	54.7
C_{16}	54.7	54.7
C_{17}	158.7	158.1

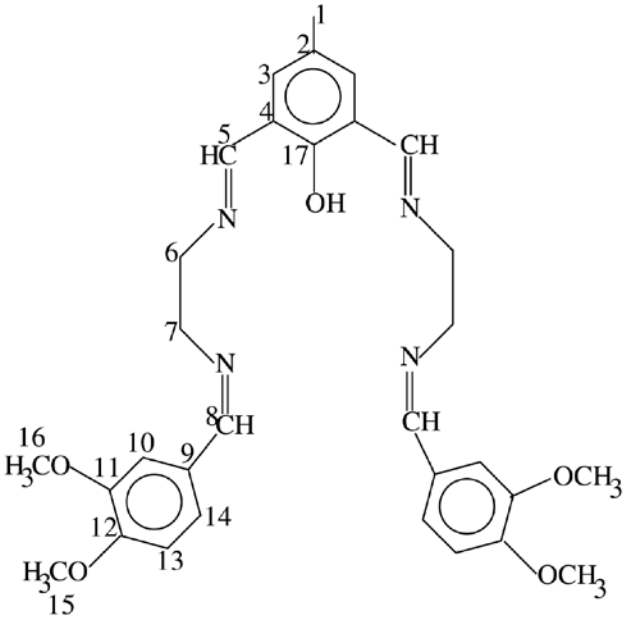

Table 2. Absorption spectral properties of synthesized complexes with DNA

Sl.No	Complexes	λmax		Δλ	Hypochromicity H	$K_b \times 10^5$
		Free	Bound	(nm)	(%)	(M^{-1})
1	$[Cu_2(BDEM)Cl_3]$	343.5	340.5	3.0	3.8	2.2
2	$[Cu_2(BHEM)Cl_3]$	355.5	350.0	5.5	6.3	2.7
3	$[Cu_2(BTEM)Cl_3]$	363.0	357.0	6.0	7.8	3.6
4	$[Zn_2(BDEM)Cl_3]$	340.0	338.0	2.0	5.6	1.6
5	$[Zn_2(BHEM)Cl_3]$	352.0	348.5	3.5	6.0	2.9
6	$Zn_2(BTEM)Cl_3]$	367.0	360.5	6.5	8.3	3.9

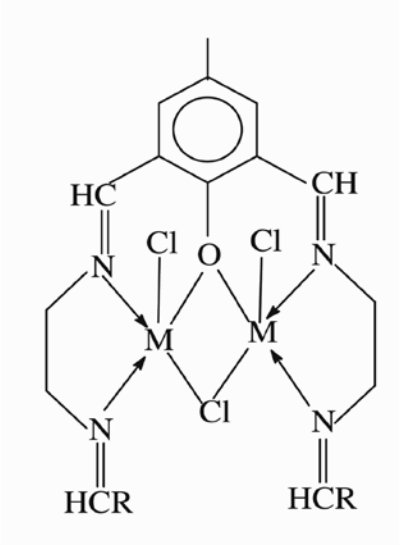

Figure 1. The proposed structure of the Schiff base complexes

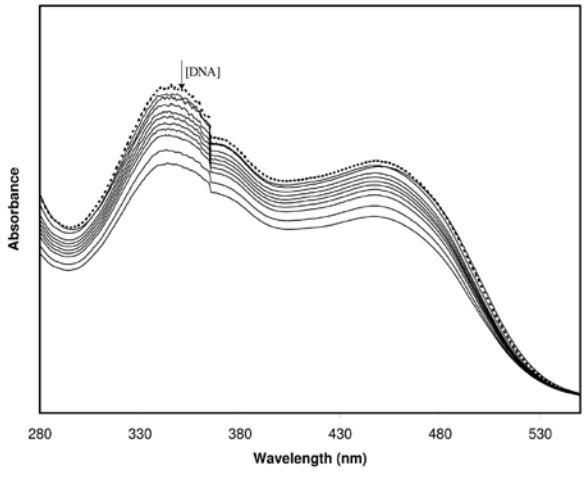

Figure 2. Electronic absorption spectrum of $[Cu_2(BDEM)Cl_3]$ in the absence (dash line) and presence (dark line) of increasing amounts of DNA

3.1.2. Viscosity measurement

Furthermore, the interactions between the complexes and DNA were investigated by viscosity measurements. Optical photophysical and voltammetry probe provided necessary, but not sufficient clues to support a binding model. Hydrodynamic measurements that were sensitive to the length change (*i.e.*, viscosity and sedimentation) were regarded as the least ambiguous and the most critical tests of binding mode in solution in the absence of crystallographic structural data [27]. A classical intercalation model usually resulted in lengthening the DNA helix as base pairs were separated to accommodate the binding ligand leading to the increase of DNA viscosity. As seen in Fig. 5, the viscosity of DNA increases with the increase in the ratio of complexes to DNA. This result further suggested an intercalative binding mode of the complex with DNA and in agreement with spectroscopic results, such as hypochromism and bathochromism of complexes in the presence of DNA.

3.1.3. Electrochemical studies

The application of cyclic voltammetry (CV) to the study of binding of metal complexes to DNA provides a useful complement to the above methods of investigations. Typical cyclic voltammograms of the $[Cu_2(BDEM)Cl_3]$ in the absence and presence of DNA are shown in Fig. 3.

In the absence of DNA, the first redox couple cathodic peak appears at 0.234 V for Cu(III) → Cu(II) (Epa = 0.573 V, Epc = 0.234 V, ΔEp = 0.339 V and $E_{1/2}$ = 0.403 V) and the second redox couple cathodic peak appears at -0.784 V for Cu(II) → Cu(I) (Epa = 0.31 V, Epc = -0.784 V, ΔEp = 0.474 V and $E_{1/2}$ = -0.237 V). In these two redox couples, the ratio of ip_c/ip_a is approximately unity. This indicates that the reaction of the complex on the gold electrode surface is a quasi-reversible redox process. The incremental addition of DNA to the complex the second redox couple causes a negative shift in $E_{1/2}$ of 37 mV and a decrease in ΔEp of 73 mV. In

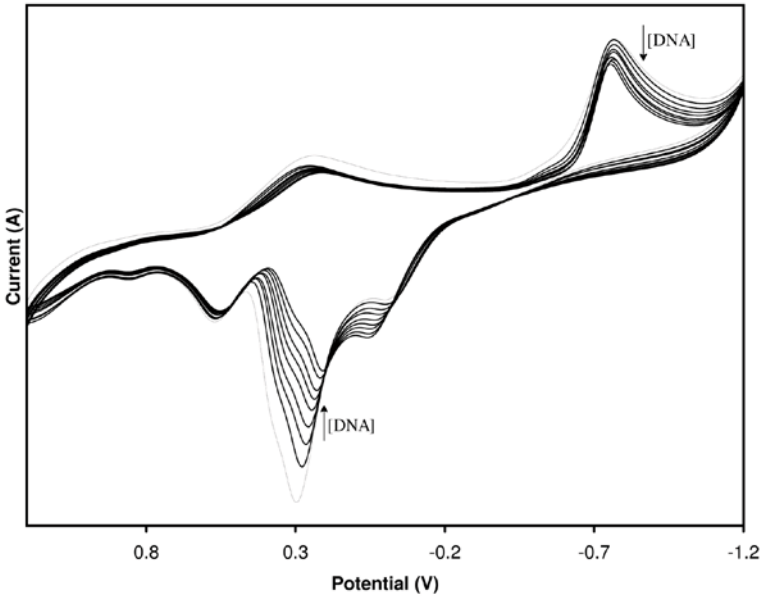

Figure 3. Cyclic voltammogram of $[Cu_2(BDEM)Cl_3]$ in the absence (dash line) and presence (dark line) of different concentration of DNA

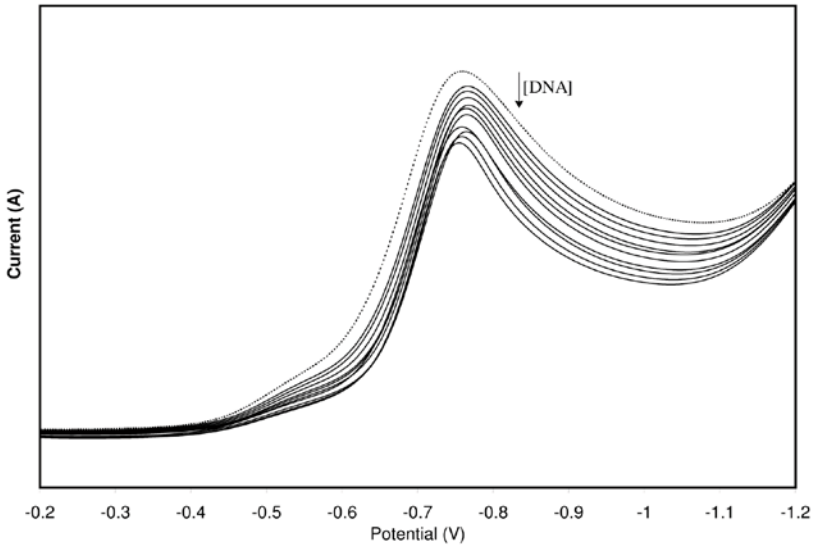

Figure 4. Differential pulse voltammogram of $[Cu_2(BDEM)Cl_3]$ in the absence (dash line) and presence (dash line) of different concentration of DNA

the presence of DNA the ip_c/ip_a values decrease in the first couple (Cu(III) → Cu(II)), but there is an increase in the ip_c/ip_a values in the second couple (Cu(II) → Cu(I)). In addition, the peak potentials, Epc and Epa, as well as $E_{1/2}$ shift to more positive values. The shift of the redox potential of the complexes in the presence of DNA to more positive values indicates a binding interaction between the complex and DNA that makes the complexes less readily reducible. The changes of the voltammetric currents in the presence of CT DNA can be attributed to diffusion of the metal complex bound to the large, slowly diffusing DNA molecule. The changes of the peak currents observed for the complexes upon addition of CT DNA may indicate that BHEM and BTEM complexes possess a higher DNA-binding affinity than the other complex. The results are similar to the above spectroscopic and viscosity data of the complexes in the presence of DNA.

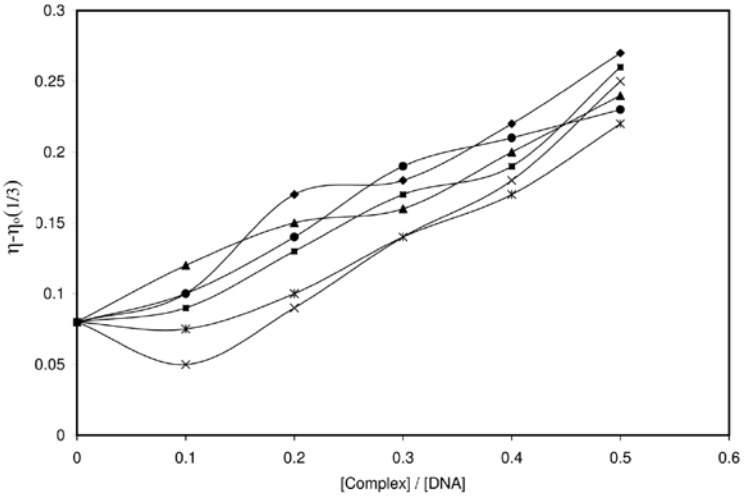

Figure 5. The effect of $[Cu_2(BDEM)Cl_3]$ (▲), $[Zn_2(BDEM)Cl_3]$ (ж), $[Cu_2(BHEM)Cl_3]$ (♦), $[Zn_2(BHEM)Cl_3]$ (●), $[Cu_2(BTEM)Cl_3]$ (×) and $[Zn_2(BTEM)Cl_3]$ (■) on the viscosity of DNA; Relative specific viscosity Vs. R = [Complex]/ [DNA]

All the zinc complexes showed a pronounced decrease in peak currents and shift in $E_{1/2}$ to less negative potential upon addition of DNA. $[Zn_2(BTEM)Cl_3]$ produced a more significant decrease in peak currents and shows a larger shift in potential upon addition of DNA. The electrochemical parameters of the Cu(II) and Zn(II) complexes are shown in Table 3 and 4 respectively. From these data it is understood that all the synthesized Cu(II) and Zn(II) complexes interact with DNA through intercalating way.

Differential pulse voltammogram of the $[Cu_2(BDEM)Cl_3]$ in the absence and presence of varying amounts of [DNA] is given in Fig. 4. Increase in concentration of DNA causes a negative potential shift along with a significant increase in current intensity. The shift in potential is related to the ratio of binding constant

$$E^{o}_{b}{}' - E^{o}_{f}{}' = 0.0591 \log (K_{+}/K_{2+}) \quad (1)$$

where $E^{o}_{b}{}'$ and $E^{o}_{f}{}'$ are formal potentials of the Cu(II)/Cu(I) complex couple in the bound and free form respectively. The ratio of the binding constants (K_{+}/K_{2+}) for DNA binding of Cu(II)/Cu(I) complexes was found to be less than unity (Table 3). This indicates that the binding of Cu(I) complex to DNA is weak compared to that of the Cu(II) complex. The above electrochemical experimental results indicate the preferential stabilization of Cu(II) form over Cu(I) form on binding to DNA.

Differential pulse voltammogram of the studied Zn(II) complexes shows a negative potential shift along with a significant decrease in current intensity during addition of increasing amounts of DNA. It indicates that zinc ions stabilize the duplex (GC pairs) by intercalating way. Hence, for the complexes of the electroactive species (Zn(II)) with DNA the electrochemical reduction reaction can be divided into two steps:

$$Zn^{2+} \text{-} DNA \rightleftharpoons Zn^{2+} + DNA$$

$$Zn^{2+} + 2e^{-} \rightleftharpoons Zn^{0}$$

Table 3. Electrochemical parameters for the interaction of DNA with Cu(II) complexes

Sl. No	Complexes	Redox couple	$E_{1/2}$ (V)		ΔEp (V)		k[red]/ k[oxd]	Ipc/Ipa
			Free	Bound	Free	Bound		
1	$[Cu_2(BDEM)Cl_3]$	Cu(III)/Cu(II)	0.403	0.503	0.339	0.345	---	0.80
		Cu(II)/Cu(I)	-0.237	-0.274	0.474	0.547	0.64	1.3
2	$[Cu_2(BHEM)Cl_3]$	Cu(III)/Cu(II)	-0.439	-0.438	0.383	0.384	---	0.75
		Cu(II)/Cu(I)	-0.600	-0.495	0.278	0.425	0.84	1.5
3	$[Cu_2(BTEM)Cl_3]$	Cu(III)/Cu(II)	-0.569	-0.544	0.097	0.074	0.72	1.4

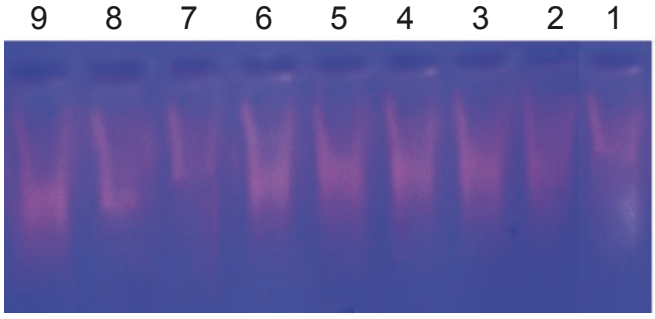

Figure 6. Gel electrophoresis diagram showing the cleavage of SC pUC 19 DNA (0.2 μg) by the synthesized complexes (50 μM) in the presence of MPA (5 mM): lane 1, DNA control; lane 2, DNA + [Cu_2(BDEM)Cl_3] + MPA; lane 3, DNA + [Cu_2(BHEM)Cl_3] + MPA; lane 4, DNA + [Cu_2(BTEM)Cl_3] + MPA; lane 5, DNA + [Zn_2(BDEM)Cl_3] + MPA; lane 6, DNA + [Zn_2(BHEM)Cl_3] + MPA; lane 7, DNA + [Zn_2(BTEM)Cl_3] + MPA; lane 8, DNA + [Cu_2(BDEM)Cl_3] + DMSO (4 μl) + MPA, lane 9, DNA + [Cu_2(BDEM)Cl_3] + distamycin (50 μM) + MPA

The dissociation constant (K_d) of the Zn(II)-DNA complex was obtained using the following equation:

$$i_p^2 = \frac{K_d}{[DNA]}\left(i_p^2{}^o - i_p^2\right) + i_p^2{}^o \quad (2)$$

where K_d is a dissociation constant of the complex Zn(II)-DNA, $i^2_p o$ and i^2_p are reduction currents of Zn(II) in the absence and presence of DNA respectively. The dissociation constant was determined using the above Eq. 2. The low dissociation constant values (Table 4) of Zn(II) ions were indispensable for catalytic function and structural stability of zinc enzymes which participate in the replication, degradation and translation of genetic material of all species.

3.2. DNA cleavage studies using Gel electrophoresis

It is known that DNA cleavage is controlled by relaxation of supercoiled circular conformation of pUC19 DNA to nicked circular and/or linear conformations. When electrophoresis is applied to circular plasmid DNA, fastest migration will be observed for DNA of closed circular conformations (Form I). If one strand is cleaved, the supercoiled will relax to produce a slower-moving nicked conformation (Form II). If both strands are cleaved, a linear conformation (Form III) will be generated that migrates in between [28].

The DNA cleavage of a ligand alone is inactive in the presence and absence of any external agents. The results indicate the importance of the metal in the complex for observing the chemical nuclease activity. The oxidative cleavage of pUC19 DNA (Fig. 6) in the presence of an external reducing agent like 3-mercaptopropionic acid (MPA, 5 mM) (type-I) has been studied by gel electrophoresis using supercoiled (SC) pUC19 DNA (0.2 µg, 33.3 µM) in 5 mM Tris–HCl/ 50 mM NaCl buffer (14 µL, pH 7.2) and the synthesized complexes (50 µM). Control experiments, using MPA or the synthesized complexes alone, show apparent cleavage of SC DNA in the absence of light. This result suggests that the synthesized complexes are able to bind to DNA. In order to determine the groove selectivity of the complexes control experiments were performed using minor groove binder distamycin. The addition of distamycin does not inhibit the cleavage for all the complexes. This indicates the major groove binding for the synthesized complexes with DNA. Control experiments show that the hydroxyl radical scavenger DMSO inhibits the DNA cleavage suggesting the possibility of hydroxyl radical and/ or ‘‘copper-oxo’’ intermediate as the reactive species [29]. SOD addition does not have any apparent effect on the cleavage activity indicating the non-involvement of the superoxide radical in the cleavage reaction. The mechanism involved in the DNA cleavage reactions is believed to be similar to that proposed by Sigman and

Table 4. Electrochemical parameters for the interaction of DNA with Zn(II) complexes

Sl.No	Complexes	Ep (V)		Ip (A)		$K_d \times 10^{-10}$ (mol L^{-1})
		Free	Bound	Free	Bound	
1	[Zn_2(BDEM)Cl_3]	-0.869	-0.801	0.205	0.151	7.2
2	[Zn_2(BHEM)Cl_3]	-0.858	-0.795	0.215	0.162	7.6
3	Zn_2(BTEM)Cl_3]	-0.847	-0.782	0.254	0.143	8.2

coworkers [30] for the chemical nuclease activity of the metal complexes.

3.2.1. Photo cleavage

Irradiation of pUC19 DNA containing Cu(II) and Zn(II) complexes was carried out in the presence and in absence of various 'inhibitors' using gel electrophoresis method. All the complexes cleave DNA from its SC to NC form, even in the absence of inhibitors, on irradiation with UV light at 360 nm. To assess the possibility that the photo-activated change involves formation of singlet oxygen and hydroxyl radical, that are responsible for the cleavage of DNA, the experiments were run in the presence of inhibitors, D_2O and DMSO. Singlet oxygen would be expected to induce more strand scission in D_2O than in H_2O, due to its longer life time in the former solvent. The same results were observed in the presence of the hydroxyl radical scavenger DMSO. Studies with singlet oxygen quencher NaN_3 were also carried out. The cleavage is slightly inhibited (Fig. 7, Lane 8) in the presence of NaN_3, which further confirmed that singlet oxygen may be the reactive species. These results indicate that, besides the presence of inhibitors, the complexes show cleavage activity upon irradiation with UV light at 360 nm.

3.3. SOD activity

The SOD mimetic activity values (IC_{50}) of synthesized complexes are given in the experimental part. In a variety of complexes which act as superoxide dismutase enzymes [31], there is either one-electron oxidation followed by reduction of a metal ion or formation of a superoxide complex which then is reduced to peroxide by another superoxide ion. In order to explore the mechanism, absorption spectrum of complexes were recorded in the presence and absence of alkaline DMSO (alkaline DMSO acts as a source of O^{2-}). The spectrum peaks became suppressed in alkaline DMSO containing buffer (pH 8.6). However upon addition of NBT, which acts as O^{2-} scavenger, these peaks were reverted to their original position. Thus, this experiment indicates that O^{2-} is initially attached to the metal complexes which later are reduced by another O^{2-} ion.

The results report the scavenging ability of each complex, giving its final concentration that produced efficient quenching of the superoxide anion radical. The lower SOD-like activity (IC_{50}) of the copper complexes is due to the weak resistance of these chelates toward the aggressive substrate O_2^- or the product O_2. The metal complexes are the most active favorably comparing with a number of synthetic SOD mimics developed for therapeutic purposes [32].

Table 5. Minimum inhibitory concentration of the synthesized compounds against the growth of four fungi (mg mL^{-1})

S.No	Compound	A. niger	A. flavus	C. albicans	R. bataicola
1	BDEM	84	73	68	64
2	BHEM	75	69	62	79
3	BTEM	82	63	73	71
4	$[Cu_2(BDEM)Cl_3]$	41	55	51	38
5	$[Cu_2(BHEM)Cl_3]$	28	32	35	33
6	$[Cu_2(BTEM)Cl_3]$	39	31	39	41
7	$[Zn_2(BDEM)Cl_3]$	27	33	42	45
8	$[Zn_2(BHEM)Cl_3]$	22	27	29	31
9	$[Zn_2(BTEM)Cl_3]$	39	49	54	57
10	Nystatin	10	8	12	14

Table 6. Minimum inhibitory concentration of the synthesized compounds against the growth of four bacteria (mg mL^{-1})

S.No	Compound	E. coli	S. typhi	S. aureus	B. subtilis
1	BDEM	60	71	67	75
2	BHEM	63	67	65	72
3	BTEM	68	74	77	80
4	$[Cu_2(BDEM)Cl_3]$	41	39	28	33
5	$[Cu_2(BHEM)Cl_3]$	22	27	17	21
6	$[Cu_2(BTEM)Cl_3]$	33	39	41	33
7	$[Zn_2(BDEM)Cl_3]$	39	34	19	37
8	$[Zn_2(BHEM)Cl_3]$	19	22	27	18
9	$[Zn_2(BTEM)Cl_3]$	33	34	37	28
10	Streptomycin	14	18	12	10

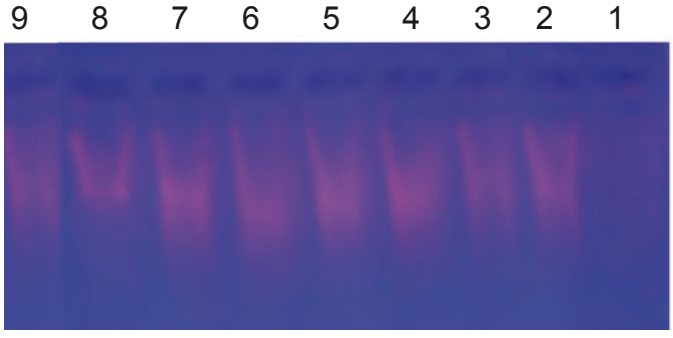

Figure 7. Gel electrophoresis diagram showing the photocleavage of pUC 19 DNA by the synthesized complexes in DMF-Tris buffer medium and in the presence of various reagents on irradiation with UV light of 360 nm: lane 1, DNA control (60 min); lane 2, DNA + $[Cu_2(BDEM)Cl_3]$ (60 min); lane 3, DNA + $[Cu_2(BHEM)Cl_3]$ (60 min); lane 4, DNA + $[Cu_2(BTEM)Cl_3]$ (60 min); lane 5, DNA + $[Zn_2(BDEM)Cl_3]$ (60 min); lane 6, DNA + $[Zn_2(BHEM)Cl_3]$ (60 min); lane 7, DNA + $[Zn_2(BTEM)Cl_3]$ (60 min); lane 8, DNA + sodium azide (100 μM) + $[Cu_2(BDEM)Cl_3]$ (30 min); lane 9, DNA + DMSO (4 μL) + $[Cu_2(BDEM)Cl_3]$ (30 min).

3.4. Antimicrobial study

For *in vitro* antimicrobial activity, the investigated compounds were tested against the above said bacteria and fungi. The minimum inhibitory concentration (MIC) values of the investigated compounds are summarized in Tables 5 and 6. A comparative study of the ligands and their complexes (MIC values) indicates that complexes exhibit higher antimicrobial activity than the free ligands. From the MIC values, it was found that the BHEM complexes are the most potent among the investigated complexes. This may be due to the electron withdrawing nature of the nitro group which enhances the positive charge on the metal ions and thereby increases the delocalization of π-electrons over the whole chelate ring and enhances the lipophilicity of the complexes. Such properties of the complexes can be explained on the basis of Overtone's [19] and Tweedy's Chelation theory [33].

4. Conclusion

Three novel Schiff base ligands and their Cu(II) and Zn(II) complexes were designed, synthesized and characterized. They have adopted bimetallic and distorted square-pyramidal/square-pyramidal geometry around the central metal ion. The binding mechanism of the complexes with DNA was not electrostatic binding but intercalation mode of binding. Noticeably, the complexes have been found to promote the cleavage of plasmid pUC19 DNA form I to form II upon irradiation. The cleavage mechanism between complexes and pUC19 DNA is likely to involve singlet oxygen and hydroxyl radicals as the reactive species. The synthesized complexes exhibit significant SOD mimetic activities. They have higher antimicrobial activity than the ligands.

Acknowledgements

The authors express their heartfelt thanks to the College Managing Board, VHNSN College, Virudhunagar for providing research facilities. NR and AS express their gratitude to the UGC, New Delhi for financial assistance.

References

[1] M. Shakir, N. Begum, Y. Azim, S. Parveen, Synth. React. Inorg. Met-Org. Chem. 33, 1367 (2003)
[2] B. Adhikari, A.K. Biswas, K. Nag, P. Zanello, A. Cinquantini, Polyhedron 6, 897 (1987)
[3] K.D. Karlin, Z. Tyeklar, In: G.L. Eichhorn, L. Marzilli (Eds.), Advances in Inorganic Biochemistry (Prentice Hall, Englewood Cliffs, NJ, 1994) Vol. 9
[4] K.D. Karluvi, Z. Tyeklar (Eds.), Bioinorganic Chemistry of Copper (Chapman and Hall, New York, 1993)
[5] A.M. Thomas, G. Neelakanta, S. Mahadevan, M. Nethaji, A.R. Chakravarty, Eur. J. Inorg. Chem. 2720 (2002)
[6] S.C. Zhang, Y. Shao, C. Tu, C.H. Dai, Z.J. Guo, Chin. J. Inorg. Chem. 20, 1159 (2004)
[7] Q.L. Li, et al., Bioorg. Med. Chem. 14, 4151 (2006)
[8] S.G. Kang, G.R. Jeong, Inorg. Chem. Commun. 12, 62 (2009)
[9] K.E. Erkkila, D.T. Odom, J.K. Barton, Chem. Rev. 99, 2777 (1999)

[10] L.J.K. Boerner, J.M. Zaleski, Curr. Opin. Chem. Biol. 9, 135 (2005)
[11] R. Bannet, Chemical Aspects of Photodynamic Therapy (Gorden and Breach, London, 2001)
[12] M.R. Detly, S.L. Gibson, S.J. Wagner, J. Med. Chem. 47, 3897 (2004)
[13] F.S. Mackay et al., Proc. Natl. Acad. Sci. USA 104, 207423 (2007)
[14] L.C. Xu, S. Shi, J. Li, S.Y. Liao, K.C. Zheng, L.N. Ji, Dalton Trans. 291 (2008)
[15] A.K. Patra, T. Bhowmick, S. Ramakumar, A.R. Chakravarty, Inorg. Chem. 46, 9030 (2007)
[16] M.J. Fernandez, B. Wilson, M. Palacios, M.M. Rodrigo, K.B. Grant, A. Lorente, Bioconjugate Chem. 18, 121 (2007)
[17] D.D. Perrin, W.L.F. Armarego, D.R. Perrin, Purification of Laboratory Chemicals (Pergamon Press, Oxford, 1980)
[18] N. Raman, S.J. Raja, J. Joseph, J.D. Raja, J. Chil. Chem. Soc. 52, 1138 (2007)
[19] A.D. Naik, V. K. Revankar, Indian J. Chem. 43A, 1447 (2004)
[20] N. Raman, A. Sakthivel, K. Rajasekaran, J. Coord. Chem. 62, 1661 (2009)
[21] N.M. Aghatabay, Y. Mahmiani, H. Cevik, B. Dulger, Eur. J. Med. Chem. 44, 365 (2009)
[22] R.G. Bhirud, T.S. Srivastava, Inorg. Chim. Acta 173, 121 (1990)
[23] M.C.R. Arguelles et al., J. Inorg. Biochem. 103, 35 (2009)
[24] S. Niu, M. Zhao, R. Ren, S. Zhang, J. Inorg. Biochem. 103, 43 (2009)
[25] B.J. Hathaway, G. Wilkinson, R.D. Gillard, J.A. McCleverty, Comprehensive Coordination Chemistry (Pergamon Press, Oxford, UK, 1987) vol. 5
[26] U. Mukhopadhyay, I. Bernal, S.S. Massoud, F.A. Mautner, Inorg. Chim. Acta 357, 3673 (2004)
[27] S. Sathyanarayana, J.C. Daborusak, J.B. Chaires, Biochemistry 32, 2573 (1993)
[28] A. Sitlani, E.C. Long, A.M. Pyle, J.K. Barton, J. Am. Chem. Soc. 114, 2303 (1992)
[29] T.B. Thederahn, M.D. Kuwabara, T.A.Larsen, D.S. Sigman, J. Am. Chem. Soc. 111, 4941 (1989)
[30] D.S. Sigman, A. Mazumder, D.M. Perrin, Chem. Rev. 93, 2295 (1993)
[31] D.T. Sawyer, J.S. Valentine, Acc. Chem. Res. 14, 393 (1981)
[32] M. Baudry, S. Etienne, A. Bruce, M. Palucki, E. Jacobsen, B. Malfroy, Biochem. Biophy. Res. Commun. 192, 964 (1993)
[33] Z.H. Chohan, H. Pervez, A. Rauf, K.M. Khan, C.T. Supuran, J. Enzy, Inh. Med. Chem. 19, 417 (2004)